Optimal Control of the Lotka-Volterra Equations with Applications

Bernard Bonnard, Jérémy Rouot

1

Optimal Control of the Lotka-Volterra Equations with Applications

Bernard Bonnard[1] and Jérémy Rouot[2]

[1] Institut Mathématique de Bourgogne, 9 rue Alain Savary, 21000 Dijon, France and Inria Sophia Antipolis. bernard.bonnard@u-bourgogne.fr
[2] Univ Brest, UMR CNRS 6205, Laboratoire de Mathématiques de Bretagne Atlantique, 6 avenue Le Gorgeu 29200 Brest jeremy.rouot@univ-brest.fr

Summary. In this article, the Lotka–Volterra model is analyzed to reduce the infection of a complex microbiote. The problem is set as an optimal control problem, where controls are associated to antibiotic or probiotic agents, or transplantations and bactericides. Candidates as minimizers are selected using the Maximum Principle and the closed loop optimal solution is discussed. In particular a $2d$–model is constructed with four parameters to compute the optimal synthesis using homotopies on the parameters. It is extended to the $3d$–case to provide a geometric frame to direct and indirect numerical schemes.

1.1 Introduction and $2d$-geometric analysis

The Lotka-Volterra equations is a model to study biological species interactions and comes from a generalization of the prey-predator model, see [21]. In this memoir the problem is already set in the control frame since the model aims to explain the evolution of two fishing species in relation with diminution of the fishing activity during the first World War.

The system is written as the 2d-dynamics:

$$\frac{\mathrm{d}N_1}{\mathrm{d}t} = N_1(\lambda_1 + \mu_1 N_2), \quad \frac{\mathrm{d}N_2}{\mathrm{d}t} = N_2(\lambda_2 + \mu_2 N_1) \tag{1.1}$$

where N_1, N_2 are the two species, $N_1, N_2 \geq 0$ and $\lambda_1, \lambda_2, \mu_1, \mu_2$ are real parameters. In the prey predator model $\lambda_1 > 0, \lambda_2 < 0, \mu_1 < 0, \mu_2 > 0$.

The system is conservative and can be integrated using the first integral:

$$\mu_2 N_1 + \lambda_2 \ln N_1 - (\mu_1 N_2 + \lambda_1 \ln N_2) = \text{constant}.$$

In the prey predator model, the evolution of each species in the quadrant $N_1, N_2 > 0$ is periodic and there exist a single persistent equilibrium: $\Omega = (K_1, K_2)$. Moreover K_1, K_2 represents the averaged population of each species on a period T

$$\langle N_i \rangle = \frac{1}{T}\int_0^T N_i(t)\mathrm{d}t = K_i,\ i = 1, 2.$$

The effect of the fishing activity is to replace:

$$\lambda_1 \to \lambda_1 - \alpha\lambda, \qquad \lambda_2 \to \lambda_2 - \beta\lambda,$$

where α, β are the modes of destruction of each species and $\lambda(t)$ is the control intensity.

Constant controls lead to shift the persistent equilibrium and hence to shift the averaged populations.

More generally the model leads to consider two vector fields (X, Y) defined by (1.1) with different parameters and to introduce the control system:

$$\frac{\mathrm{d}x(t)}{\mathrm{d}t} = u(t)X(x(t)) + (1 - u(t))Y(x(t)),$$

$x = (N_1, N_2)$ and $u \in [0, 1]$.

The Lotka–Volterra equations can more generally described the interaction of n-species $x = (x_1, \ldots, x_n)^\intercal$, $x_i \geq 0$, and is given by the dynamics:

$$\frac{\mathrm{d}x}{\mathrm{d}t} = (\mathrm{diag}x)(Ax + r), \tag{1.2}$$

where $\mathrm{diag}x$ is the diagonal matrix with entries $(x_1, \ldots, x_n)$, $A = (a_{ij})$ is the matrix of interaction coefficients and $r = (r_1, \ldots, r_n)^\intercal$ is the vector of individual growth of the species. Recently based on the model of [20] of the intestinal microbiote with $n = 11$ species, Jones et al. [13] analyzed the problem of reducing C. difficile infection (a pathogenic agent) using either antibiotic or fecal transplantation.

Denoting by $X(x) = (\mathrm{diag}x)(Ax+r)$ the n-dimensional dynamics ($n = 11$) with parameters given in [20], the control system writes as:

$$\frac{\mathrm{d}x(t)}{\mathrm{d}t} = X(x(t)) + u(t)Y(x(t)) + \sum_{i=1}^{k} \lambda_i \delta(t - t_i)Y'(x)), \tag{1.3}$$

where $Y(x) = (\mathrm{diag}x)\boldsymbol{\epsilon}$, $\boldsymbol{\epsilon} = (\varepsilon_1, \ldots, \varepsilon_n)$ is the sensitivity vector to the antibiotic of the species and $u(t)$ is a piecewise constant mapping. The second control action is associated to jumps $x(t_i) \to x(t_i) + \lambda v$ in the state, and $Y'(x) = v$, corresponding to ratio of each species in the transplantation.

Denoting by x_1 the C. difficile population, the optimal control problem can be set as a Mayer problem: $\min x_1(t_f)$ where t_f is the number of days of the treatment or in a dual form: reach in minimum time t_f a specific level d of infection that is: $x_1(t_f) = d$.

The optimal control problem can be posed in the general frame of mixing permanent controls associated to antibiotic treatment or sampled-data controls associated to transplantations.

In both case the optimal control problem can be analyzed with an indirect scheme based on the Maximum Principle [17] in the permanent case or an adaptation in the sampled-data control case, or by a direct numerical optimization scheme.

In this article, the starting point is to analyze the effect of an antibiotic or probiotic treatment restricting to a control system of the form:

$$\frac{\mathrm{d}x(t)}{\mathrm{d}t} = X(x(t)) + u(t)Y(x(t)),$$

with $x(t) \in \mathbb{R}^n$, the set of admissible controls $\mathcal{U}$ being the set of measurable mappings valued in $]-1,+1[$ (for convenience we assume $u = -1$ being associated to no treatment, $u = +1$ to maximum dosing regimen). We consider the problem of steering $x(0) = x_0$ to a terminal manifold N of codimension one, e.g.: $x_1 = d$, in minimum time. We mainly focus our study the the $2d$–case.

Our analysis is based on a series of recent articles [4, 15, 5] to classify the closed loop optimal solutions in a neighborhood of the terminal manifold, using semi-normal forms for the triple (X, Y, N), under generic assumptions. They can be globalized in the frame of polynomic systems using homotopies on the parameters.

It is completed in the $3d$–case by direct and indirect numerical schemes to provide robust optimal controls taking into account the combination of various treatments and medical logistical constraints [2, 8, 18] using preliminary geometric analysis.

1.2 The Maximum Principle in the permanent case and the classification of the extremals

1.2.1 Maximum Principle

Denote $F(x,u) = p \cdot (X(x) + uY(x))$ and $H = p \cdot F(x,u)$ the Hamiltonian lift defining the pseudo-Hamiltonian, $p \in \mathbb{R}^n \setminus \{0\}$ being the adjoint vector. If $(x(.), u(.))$ is optimal on $[0, t_f]$ then there exists $(z(.), u(.))$, $z = (x, p)$ such that a.e. :

$$\begin{aligned} \frac{\mathrm{d}x}{\mathrm{d}t}(t) &= \frac{\partial H}{\partial x}(x(t), p(t), u(t)), \\ \frac{\mathrm{d}p}{\mathrm{d}t}(t) &= -\frac{\partial H}{\partial p}(x(t), p(t), u(t)). \end{aligned} \tag{1.4}$$

Moreover the optimal control satisfies a.e. the maximization condition

$$H(z(t), u(t)) = \max_{|v| \leqq 1} H((z(t)), v) = M(z(t)), \tag{1.5}$$

where $M((z(t)) \geq 0$ is constant.

At the final time the transversality condition is satisfied:

$$p(t_f) \perp T^*_{x(t_f)} N. \tag{1.6}$$

Definition 1. *An extremal* (z,u) *is a solution of* (1.4)-(1.5) *on* $[0,t_f]$. *It is called a BC–extremal if the transversality condition* (1.6) *is satisfied. An extremal is called regular if a.e.* $u(t) = \text{sign}H_Y(z(t))$ *and singular if* $H_Y(z(t)) = 0$ *identically. A regular extremal is called bang-bang (BB) if the the number of switches is finite. An extremal* (x,p,u) *is called strict if* $p(.)$ *is unique up to a factor.*

1.2.2 Small time classification of regular extremals near the switching surface.

One needs the following see [14] for the details.

Let $t \to z(t)$ be a regular extremal on $[0,t_f]$ and we denote by $t \to \Phi(z(t)) = H_Y(z(t))$ the switching function and let Φ_ε the switching function along a bang arc extremal with $u = \varepsilon = \pm 1$ constant. We denote respectively by σ_+, σ_-, bang arcs with $u = \pm 1$ and σ_s a singular arc, while $\sigma_1\sigma_2$ denotes a σ_1 arc followed by an σ_2 (where each arc of the sequence can be empty). We denote by Σ the switching surface $H_Y(z) = 0$ and Σ' the subset $H_Y(z) = \{H_Y, H_X\}(z) = 0$. The Lie bracket of two vector fields Z_1, Z_2 being computed with the convention $[Z_1,Z_2](x) = \frac{\partial Z_1}{\partial x}(x)Z_2(x) - \frac{\partial Z_2}{\partial x}(x)Z_1(x)$. If $H_i(z) = p\cdot Z_i(x)$ the Poisson bracket is $\{H_1,H_2\} = \mathrm{d}H_1(\boldsymbol{H}_2) = p\cdot[Z_1,Z_2](x)$, where $\boldsymbol{H}_2 \coloneqq (\nabla_p H_2, -\nabla_x H_2)$ is the Hamiltonian vector field.

Deriving twice the switching function $\Phi(t)$ one gets:

$$\begin{aligned} &\frac{\mathrm{d}\Phi}{\mathrm{d}t}(t) = \{H_Y,H_X\}(z(t)),\\ &\frac{\mathrm{d}^2\Phi}{\mathrm{d}t^2}(t) = \{\{H_Y,H_X\},H_X\}(z(t)) + u(t)\{\{H_Y,H_X\},H_Y\}(z(t)). \end{aligned} \tag{1.7}$$

Let t be a switching time so that $\Phi(t) = 0$ and assume that at $z(t)$ the surface Σ' is regular.

Proposition 1. *Assume that the switching time* t *is ordinary that is:* $\Phi(t) = 0$ *and* $\frac{\mathrm{d}\Phi}{\mathrm{d}t}(t)$ *is non zero. Then near* $z(t)$ *every extremal projects onto* $\sigma_+\sigma_-$ *if* $\frac{\mathrm{d}\Phi}{\mathrm{d}t}(t) > 0$ *or* $\sigma_-\sigma_+$ *if* $\frac{\mathrm{d}\Phi}{\mathrm{d}t}(t) < 0$.

Proposition 2. *Assume that at the switching time* t, *the switching function* $\Phi_\varepsilon(t)$ *for* $u = \varepsilon = \pm 1$ *is such that* $\frac{\mathrm{d}\Phi_\varepsilon}{\mathrm{d}t}(t) = 0$ *and both* $\frac{\mathrm{d}^2\Phi_\varepsilon}{\mathrm{d}t^2}(t) \neq 0$ *where the second order derivative is given by* (1.7). *Then* $z(t)$ *is called a fold point and we have:*

- *In the parabolic case:* $\frac{\mathrm{d}^2\Phi_+}{\mathrm{d}t^2}(t)\cdot\frac{\mathrm{d}^2\Phi_-}{\mathrm{d}t^2}(t) > 0$, *each extremal near* $z(t)$ *projects onto* $\sigma_\pm\sigma_\pm\sigma_\pm$.
- *In the hyperbolic case:* $\frac{\mathrm{d}^2\Phi_+}{\mathrm{d}t^2}(t) > 0$, $\frac{\mathrm{d}^2\Phi_-}{\mathrm{d}t^2}(t) < 0$ *it projects onto* $\sigma_\pm\sigma_s\sigma_\pm$.
- *In the elliptic case* $\frac{d^2\Phi_+}{\mathrm{d}t^2}(t) < 0$, $\frac{\mathrm{d}^2\Phi_-}{\mathrm{d}t^2}(t) > 0$, *every extremal is bang-bang but the number of switches is not uniformly bounded.*

1.2.3 Computations of the singular extremals with minimal order

The computations is standard, see [3]. Derive twice with respect to time $H_Y(z(t)) = 0$ one gets

$$\begin{aligned} &H_Y(z(t)) = \{H_Y, H_X\}(z(t)) = 0, \\ &\{\{H_Y, H_X\}, H_X\}(z(t)) + u_s(t)\{\{H_Y, H_X\}, H_Y\}(z(t)) = 0. \end{aligned} \tag{1.8}$$

Assume the generalized Legendre-Clebsch condition $\{\{H_Y,H_X\},H_Y\}(z(t)) \neq 0$ holds for every t then from equation (1.8), $u_s(t) = u_s(z(t))$ is the dynamic feedback:

$$u_s(z) = -\frac{\{\{H_Y, H_X\}, H_X\}(z)}{\{\{H_Y, H_X\}, H_Y\}(z)}$$

and plugging such u_s in the pseudo-Hamiltonian defines the true Hamiltonian:

$$H_s(z) = H_X(z) + u_s(z)H_Y(z).$$

Hence we deduce:

Proposition 3. *Singular extremals with minimal order* $\{\{H_Y, H_X\}, H_Y\}(z) \neq 0$ *are solutions of the Hamiltonian dynamics* $\boldsymbol{H}_s(z)$ *restricted to the invariant surface* Σ'*:* $H_Y(z) = \{H_Y, H_X\}(z) = 0$*.*

Definition 2. *Assume that we are in the strict case. Since the true Hamiltonian is constant then the singular trajectories projections of singular extremals of minimal order are stratified according to the following:*

- *Hyperbolic case:* $H_X(z).\{\{H_Y, H_X\}, H_Y\}(z) > 0$*,*
- *Elliptic case:* $H_X(z).\{\{H_Y, H_X\}, H_Y\}(z) < 0$*,*
- *Abnormal or exceptional case:* $H_X(z) = 0$*.*

1.2.4 Construction of the optimal synhesis in a neighborhood of N

Take a point x_0 which can be identified to 0. Assume that at such point the surface N is regular. We denote by $N^\perp$ the Hamiltonian lift: $\{z = (x, p); x \in N, p = n(x)\}$ where n is the normal to N at x.We shall assume that the cone of limit directions $\{X \pm Y\}$ is strict and one can suppose it is contained in an half-space, so that n can be chosen assuming $n(x) \cdot X(x) > 0$.

If $n(x) \cdot Y(x) \neq 0$,then every extremal near N is determined by the transversality condition: $u = +1$ if $n \cdot Y > 0$ and $u = -1$ otherwise. Switches can occur only near points such that Y is tangent to N, that is $n \cdot Y(x) = 0$.

The regular synthesis [10] amounts to compute in a neighborhood U of x_0, in the domain $n \cdot X(x) < 0$ the following strata:

- The switching locus W restricting to ordinary switches with strata W_+, W_- corresponding respectively to $\sigma_-\sigma_+$ or $\sigma_+\sigma_-$, and associated to optimal policies only.

- The set Σ_s filled by optimal $BC-$ singular arcs.
- The cut locus C defined as follows. Every optimal arc $\sigma(t)$ is integrated backwards in time, that is $\sigma(t)$ is defined on $[t_f, 0]$ so that $t_f < 0$ and $\sigma(0) \in N$. The cut locus is the closure of the set of points $z(t_c)$, $t_f < t_c < 0$ so that $z(t)$ is not optimal beyond the time t_c. It contains the separating locus formed by the set of points where there exits two distinct minimizers reaching N.

The contribution of the series of papers [4, 15, 5] describes the time minimal syntheses for all cases of codimension ≤ 2 in the jet spaces of the triples (X, Y, N) at $x_0 = 0$. We shall present the main application, restricting to the $2d$–case for the controlled Lotka-Volterra model, to describe geometrically the main features of the time minimal syntheses.

1.3 The geometric determination of the time minimal syntheses for the Lotka-Volterra model – $2d$-case

1.3.1 Determination of the collinearity locus in relation with forced permanent equilibria

Plugging $u = \pm 1$ leads to forced equilibria with constant dosing regimen associated to no treatment with $u = -1$ and maximal dosing regimen with $u = +1$.

Hence in the n-dimensional case we introduce the collinearity locus as the one-dimensional variety defines as projection on the state space of the set:

$$\{(x_e, \lambda) \in \mathbb{R}^{n+1}; \lambda = -u_e, X(x_e) = \lambda Y(x_e)\}.$$

The constant control u_e is such that (x_e, u_e) is a forced equilibrium and it has to be feasible that is $|u_e| \leq 1$.

Following Volterra [21] one can choose for each dynamics $(\mathrm{diag}x)(Ax + r)$ dimensionless coordinates so that up to translation the dynamics takes the form $-\mathrm{diag}(x+1)A^*x$, where the persistent equilibrium is identified to 0 and the spectrum of the linearized dynamics is given by $-\sigma(A^*)$ with $\sigma(A^*) = \{\lambda_1, \ldots, \lambda_n\}$ where each λ_i denotes an eigenvalue, with generalized eigenspace E_{λ_i}.

In the 2d-case the computation of the collinearity locus is simple and is the determinantal set

$$\mathcal{C} = \det(X(x), Y(x)) = 0.$$

Straightforward computations define a segment L_1 when restricting to the persistent quadrant: $x_1, x_2 > 0$. Furthermore a subsegment L_1' is defined due to the control restriction $|u_e| \leq 1$.

Each point of this segment determines a forced equilibrium with a corresponding spectra.

Example 1. Consider the conservative case described by (1.1) with parameters $(\lambda_1, \lambda_2, \mu_1, \mu_2)$ and $\Omega = (K_1, K_2)$ be the persistent equilibrium. The dynamics can be set in normalized coordinates introducing $n_i = \frac{N_i}{K_i}$ and $n_i \to n_i - 1$ so that it takes the form: $-\mathrm{diag}(x+1)A^*x$. Choosing Ω in the quadrant $N_i > 0$ imposes constraints: $\lambda_1\mu_1 > 0$ and $\lambda_2\mu_2 < 0$. One can choose the ratio $\lambda = \lambda_2/\mu_2$ as an homotopy parameter and consider the one-dimensional dynamics $\lambda \to (\mathrm{diag}x)(A(\lambda)x + r(\lambda))$ where λ can be restricted to a segment.

1.3.2 Determination of the singular locus

In the $2d$–case, using $H_Y(z) = \{H_X, H_Y\}(z) = 0$, the singular locus is the determinantal set $\mathcal{S}$ defined by:

$$\det(Y(x), [Y, X](x)) = 0.$$

In the persistent space they formed a line passing through the origin.

For some parameters value, the collinear and singular loci intersects at a single point denoted O. The main point of this section will be to discuss the construction of the time minimal synthesis in a neighborhood of O, illustrating the applications of the concepts and techniques from [4, 15, 5]. This will lead to identify four parameters to construct the global syntheses by homotopy. The geometric schematic picture is represented on Fig.1.1 where we have reported symbolically on the extremities of the collinear locus the two cases studied by Volterra [21], illustrating clearly the global issues.

In the $2d$-case, much information about the global synthesis can be deduced using the clock form one-form ω defined outside the collinearity locus by the relations:

$$\omega(X) = p \cdot X(x) = 1, \quad \omega(Y) = p \cdot Y(x) = 0.$$

Green's theorem allows to deduces optimality status of $\sigma_+\sigma_-$ vs $\sigma_-\sigma_+$, in different domains, observing that $\mathrm{d}\omega$ vanishes precisely on the singular locus.

Since Lie brackets have complicated values, the use of a semi-normal form for the actions of local changes of coordinates and feedbacks $u \to -u$ aims to simplify the computations.

In particular, such a construction will be useful to deduce the time minimal synthesis in a neighborhood of 0 and identify the homotopy parameters to construct the global synthesis.

Construction of the semi-normal form

First of all, one can choose coordinates such that $O = (0, 0)$ and Y is identified to the vector field $Y = \frac{\partial}{\partial x_2}$ (this amounts mainly to choose ln-coordinates), furthermore the singular direction can be identified to the axis (Ox_1).

Expanding X in the jet space at $O = (0, 0)$, this leads to analyze the control system:

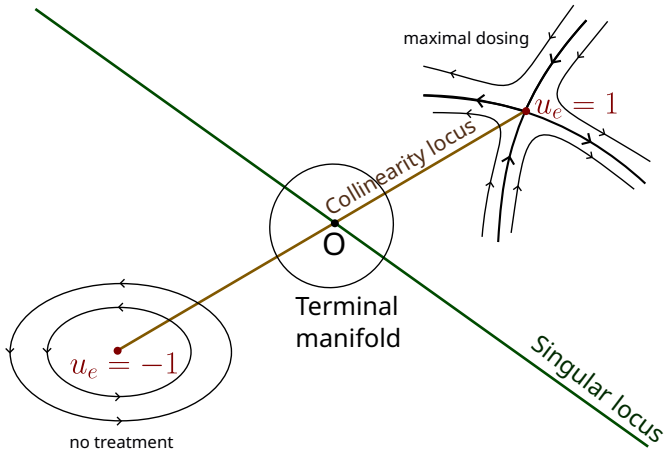

Fig. 1.1. Schematic representation of a case study: end–points of the collinear locus and intersection of the singular and collinear locus.

$$\frac{\mathrm{d}x_1}{\mathrm{d}t} = -\lambda x_1 + \alpha x_2^2, \frac{\mathrm{d}x_2}{\mathrm{d}t} = (u - u_e),$$

with $u_e \in]-1, +1[$, $\mid u \mid \leq 1$ and $\alpha > 0$.

Properties of the system

Computing Lie brackets in those coordinates shows relevant simplifications:

- $X(x) = (-\lambda x_1 + \alpha x_2^2)\frac{\partial}{\partial x_1} - u_e \frac{\partial}{\partial x_2}$,
- $Y(x) = \frac{\partial}{\partial x_2}$,
- $[Y, X](x) = -2\alpha x_2 \frac{\partial}{\partial x_1}$,
- $[[Y, X], Y](x) = -2\alpha \frac{\partial}{\partial x_1}$.

Hence the singular line is given by: $x_2 = 0$ and restricting to this line one has:

$$X(x_1) = -\lambda x_1 \frac{\partial}{\partial x_1}, \quad [[Y, X], Y](x_1) = -2\alpha \frac{\partial}{\partial x_1}.$$

Therefore for the restriction one has:

$$[[Y, X], Y](x_1) = \frac{2\alpha}{\lambda} X(x_1).$$

Then we have:

- The origin is an abnormal singular arc reduced to a point and the subarc of the line $x_2 = O$ is hyperbolic in $x_1 > 0$ and the subarc is elliptic if $x_1 < 0$.
- The singular control along the line $x_2 = 0$ is given by: $u = u_e$ and is constant and strictly admissible if $u_e \in]-1, +1[$.

- The collinear set is given by the parabola: $x_1 = \frac{\alpha x_2^2}{\lambda}$.
- The clock form is: $\omega = \frac{\mathrm{d}x_1}{(-\lambda x_1 + \alpha x_2^2)}$.

Moreover for every constant control $u = \varepsilon,\ \varepsilon = \pm 1$, the extremal system can be integrated.

One can construct a case study taking as terminal manifold N a circle centered at O=$(0,0)$, with radius d intersecting the singular line at $(\pm d, 0)$. The time minimal synthesis outside the disk and near the two points $(\pm d, 0)$ can be directly deduced from the classification of [5], thanks to the curvature of the terminal manifold in the chosen normal coordinates. It is represented on Fig.1.2 and we have:

- *Top:* $(-d, 0)$ lifts into a fold elliptic point. The singular line is time maximizing. The optimal policy is $\sigma_+\sigma_-$ or $\sigma_-\sigma_+$ using the clock form and we have represented the two strata of the switching locus: $W = W_- \cup W_+$ and there exists a cut locus C. The three curves of the stratification are ramifying at $(-d, 0)$.
- *Bottom:* $(d, 0)$ lifts into an hyperbolic fold point and the time minimal synthesis is of the form: $\sigma_-\sigma_s$ or $\sigma_+\sigma_s$.

To construct the complete synthesis one must glue the two cases along the exterior of the circle and fill the interior of the disk.

To simplify the computations, we have assume that $u_e = 0$. The synthesis is represented on Fig.1.3.

Note that the singular line prolongated onto a cut locus terminating at $(d, 0)$. In the non symmetric case $u_e \neq 0$, the cut locus persists but is not coinciding with this segment.

In this synthesis we assume that the two points $(\pm d, 0)$ lift into fold points. But clearly we can obtain more general cases unfolding the syntheses with a parameter w by taking the system

$$\frac{\mathrm{d}x_1}{\mathrm{d}t} = -\lambda x_1 + w x_2 + \alpha x_2^2, \frac{\mathrm{d}x_2}{\mathrm{d}t} = (u - u_e),$$

where w is a constant.

This leads to unfold the synthesis as represented on figs. 1.4-1.5. Note that the sign of w is not relevant in the pictures since one can change u into $-u$ in the computations.

The switching locus W can be evaluated expanding the switching function, where the expansions are described in [5] and are in any case of order at most 2.

1.3.3 Computations on the 2*d*–model

In this section we present direct computations on the $2d$-model vs the use of the semi-normal form. To simplify the notations we note (x, y) the $2d$-coordinates so that one has:

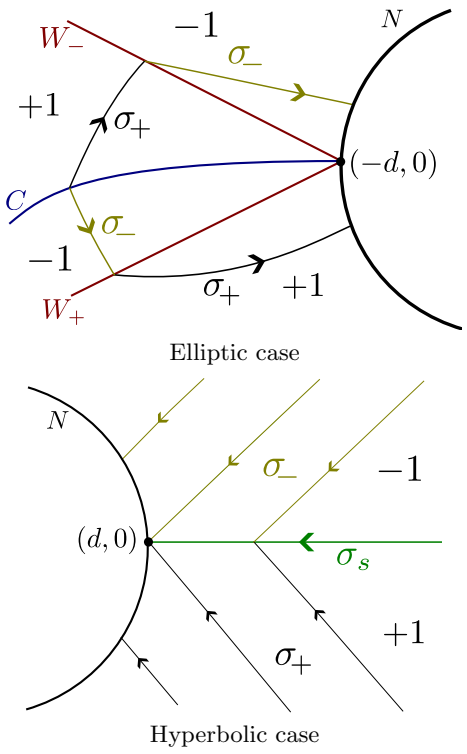

Fig. 1.2. $2d$–syntheses near $(\pm d, 0)$ outside the disk.

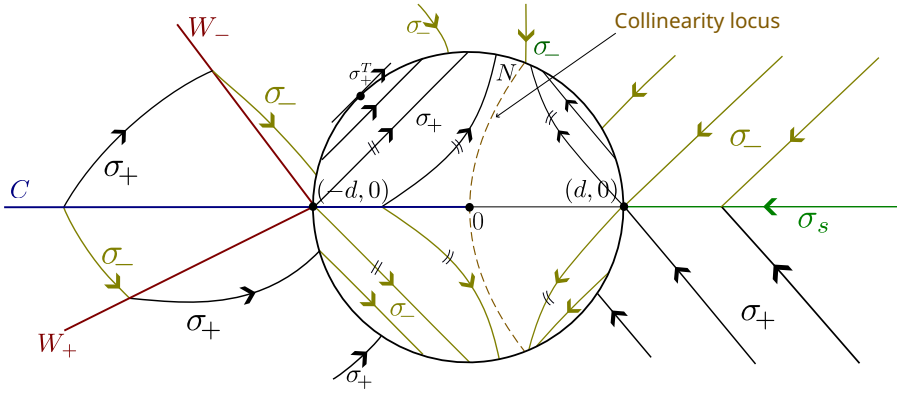

Fig. 1.3. Gluing hyperbolic and elliptic case with N being a circle; the symmetric case $u_e = 0$.

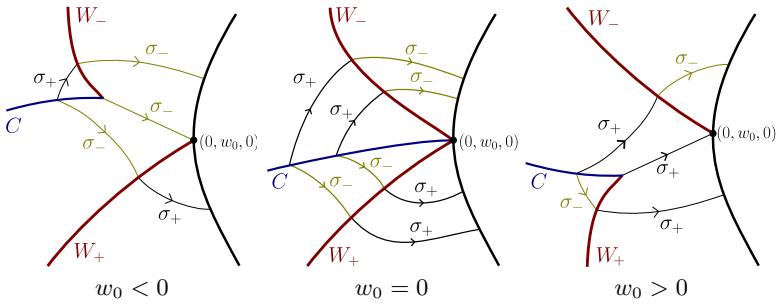

Fig. 1.4. Unfolding with parameter w_0 in the elliptic case.

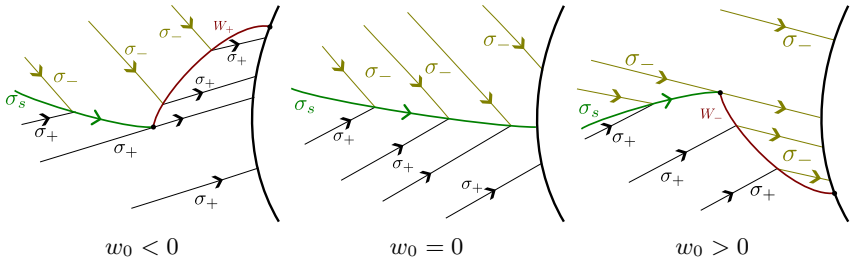

Fig. 1.5. Unfolding with parameter w_0 in the hyperbolic case.

$$X = (x(r_1 + a_{11}x + a_{12}y), y(r_2 + a_{21}x + a_{22}y))^\intercal,$$
$$Y = (x\varepsilon_1, y\varepsilon_2)^\intercal.$$

Using ln–coordinates it takes the form:

$$X = ((r_1 + a_{11}e^x + a_{12}e^y), (r_2 + a_{21}e^x + a_{22}e^y))^\intercal,$$
$$Y = (\varepsilon_1, \varepsilon_2)^T.$$

Lie brackets are invariant and can computed in such coordinates which simplify the calculations since the vector field Y becomes constant.

Moreover one can impose in the class two geometric normalizations to clarify the analysis.

Normalizations

- One can suppose that the persistent equilibrium is $\Omega = (1, 1)$.
- One can assume that the persistent singular locus is the line: $y = x$.

This leads respectively to:

$$r_1 = -(a_{11} + a_{12)}, r_2 = -(a_{21} + a_{22}), \tag{1.9}$$

and

$$\varepsilon_1(\varepsilon_2 a_{11} - \varepsilon_1 a_{21}) = \varepsilon_2(\varepsilon_1 a_{22} - \varepsilon_2 a_{12}). \tag{1.10}$$

Lie brackets are given by:

$$[X,Y] = (x(\varepsilon_1 a_{11}x + \varepsilon_2 a_{12}y), y(\varepsilon_1 a_{21}x + \varepsilon_2 a_{22}y))^\intercal,$$
$$[[Y,X],Y] = (-x(\varepsilon_1^2 a_{11}x + \varepsilon_2^2 a_{12}y), -y(\varepsilon_1^2 a_{21}x + \varepsilon_2^2 a_{22}y))^\intercal,$$

the Lie bracket $[[X,Y],X]$ is more complex and takes in ln–coordinates the form:

$[[Y,X],X] = ((\varepsilon_1 a_{11}e^x(r_1 + a_{12}e^y) + \varepsilon_2 a_{12}e^y(r_2 + a_{21}e^x) - a_{11}e^x\varepsilon_2 a_{12}e^y - a_{12}e^y\varepsilon_1 a_{21}e^x), (\varepsilon_1 a_{21}e^x(r_1 + a_{12}e^y) + \varepsilon_2 a_{22}e^y(r_2 + a_{21}e^x) - a_{21}e^x\varepsilon_2 a_{12}e^y - a_{22}e^y\varepsilon_1 a_{21}e^x))^\intercal$.

One introduces the following determinants:

$$D = \det(Y,[[Y,X],Y]),$$
$$D' = \det(Y,[[Y,X],X]), \qquad D'' = \det(Y,X).$$

The generalized Legendre-Clebsch condition holds if along the singular line $y = x$,

$$D = xy[\varepsilon_1^2 x(\varepsilon_2 a_{11} - \varepsilon_1 a_{21}) + \varepsilon_2^2 y(\varepsilon_2 a_{12} - \varepsilon_1 a_{22})]$$

is non zero.

This gives restricting to $y = x$,

$$\frac{D}{xy} = xC,$$
$$C = \varepsilon_1^2(\varepsilon_2 a_{11} - \varepsilon_1 a_{21}) + \varepsilon_2^2(\varepsilon_2 a_{12} - \varepsilon_1 a_{22}) \neq 0.$$

Using the normalization condition (1.10) we get the condition

$$(\varepsilon_1\varepsilon_2 - \varepsilon_2^2)(\varepsilon_1 a_{22} - \varepsilon_2 a_{12}) \neq 0.$$

The singular control along the singular line $y = x$ is given by:

$$u_s = -\frac{D'_{|y=x}}{D_{|y=x}}.$$

Computing D' restricted to $y = x$ leads to introduce the coefficients:

$A = \varepsilon_1\varepsilon_2 a_{11}r_1 + \varepsilon_2^2 a_{12}r_2 - \varepsilon_1^2 a_{21}r_1 - \varepsilon_1\varepsilon_2 a_{22}r_2$,

$B = \varepsilon_1\varepsilon_2 a_{11}a_{12} + \varepsilon_2^2 a_{12}a_{21} - \varepsilon_2^2 a_{11}a_{12} - \varepsilon_1\varepsilon_2 a_{12}a_{21} - \varepsilon_1^2 a_{21}a_{22} - \varepsilon_1\varepsilon_2 a_{21}a_{22} + \varepsilon_1\varepsilon_2 a_{21}a_{12} + \varepsilon_1^2 a_{22}a_{21}$. Hence the first component (projecting on the $x-axis$) of $-u_sY$ restricting to the singular line $y = x$ takes the form

$$-\frac{(A + Bx)}{C}\varepsilon_1 x.$$

It has to vanishes at $x = 1$, so that $B = -A$. The derivative at $x = 1$ is $\frac{-\varepsilon_1(A+2B)}{C} = \frac{\varepsilon_1 A}{C}$.

Similarly at $\Omega = (1, 1)$, X has to vanishes, which corresponds to (1.9) and the derivative at $x = 1$ is $-r_1$.

Hence the dynamics along the singular line at $x = 1$ is regular if

$$-r_1 + \varepsilon_1 \frac{A}{C} \neq 0. \tag{1.11}$$

Note that we can reverse the orientation on the singular line changing in the same category X into $-X$.

In particular one deduces the following:

Theorem 1. *Under regularity conditions previously described, the singular flow along the singular line belongs to the one dimensional Lotka–Volterra form:* $\frac{\mathrm{d}x}{\mathrm{d}t} = x(r + ax)$ *and at the persistent equilibrium point the eigenvalue of the linearized dynamics is given by* $-r_1 + \varepsilon_1 \frac{A}{C}$.

1.3.4 Conclusion

Our study shows the main features to compute time minimal syntheses in different neighborhood of the origin and with different terminal manifolds. The main singularity is the interaction between the collinearity and the singular loci. We have introduced a semi-normal form with four homotopy parameters describing the main features of the geometric construction. Different cases can be analyzed gluing different syntheses. In particular the detailed computations of Section 1.3.3 show the role of the singular locus to extend the synthesis for large times.

1.4 From $2d$–case to $3d$–case and numerical simulations

1.4.1 The geometric frame

In this section we consider a $3d$ controlled Lotka–Volterra dynamics of the form

$$\frac{\mathrm{d}x}{\mathrm{d}t}(t) = X(x(t)) + \sum_{i=1}^{2} u_i(t) Y_i(x(t)),\ x = (x_1, x_2, x_3)^\intercal \in K \coloneqq \mathbb{R}^3_+, \tag{1.12}$$

where x_1 is the infected population and $u = (u_1, u_2),\ 0 \leq u_1 \leq 1, 0 \leq u_2 \leq 1 + \varepsilon,\ \varepsilon > 0$.
In this control system,

- X stands for the non controlled Lotka-Volterra dynamics given by $X = \mathrm{diag}x(Ax + r)$,
- $Y_1 = \mathrm{diag}x\ \epsilon$, ϵ is the constant sensitivity vector associated to a probiotics $\epsilon = (\varepsilon_1, \varepsilon_2, \varepsilon_3)^\intercal$, $\varepsilon_i \geq 0,\ i = 1, 2, 3$.

- $Y_2 = \mathrm{diag}x\ \epsilon$', ϵ' is the constant sensitivity vector associated to an antibiotic $\epsilon' = (\varepsilon'_1, \varepsilon'_2, \varepsilon'_3)^\intercal$, $\varepsilon'_i \leq 0,\ i = 1, 2, 3$.

Our aim is to reduce the x_i-population using the following protocol:

- Prior to infection use the probiotic to reinforce the microbiote.
- Having detected a given level of infection, reach in minimum time a forced equilibrium associated to a given level of infection. Moreover this level has to be stabilisable.

1.4.2 A rough classification of Lotka–Volterra dynamics

Definition 3. *We restrict to the case $r_i > 0,\ i = 1, 2, 3$ so that the origin O is a repeller and there exist axial equilibria $e_1 = (1, 0, 0)^\intercal$, $e_2 = (0, 1, 0)^\intercal$ and $e_3 = (0, 0, 1)^\intercal$. The system is called totally competitive if for all $1 \leq i, j \leq 3,\ a_{ij} < 0$. Additional equilibria may exist in the cone K and are denoted respectively : interior equilibrium Ω and $E_{jk},\ j < k$ related to extinction of species $i \neq j, k$.*

One has the following result from [1].

Proposition 4. *In the totally competitive case, there exists an unique Lipschitz invariant manifold Π that attracts $K\backslash\{0\}$ and every trajectory in $K\backslash\{0\}$ is asymptotic to one in Π. The manifold Π is homeomorphic to the closed unit simplex $S = \{x \geq 0,\ x_1 + x_2 + x_3 = 1\}$ under radial projection. Moreover the boundary of the basin of repulsion of the origin coincides with Π.*

Proposition 5. *The system obtained by adding a probiotic vector fields to a totally competitive system is also totally competitive. The same holds for antibiotic provided $|u_2|$ is small enough.*

1.4.3 Construction of the carrying simplex

The following is crucial for numeric computation of Π. We denote by $\varphi_t,\ t \geq 0$ the positive semi–flow generated by the Lotka–Volterra dynamics and M_t is the image by φ_t of the triangle S whose vertex are the three axial equilibria.

Proposition 6. *In the totally competitive case the sequence of surfaces (with corners) M_t converges uniformly to Π as t tends to $+\infty$.*

Remark 1. The interesting point is in a more general context to evaluate the boundary of the basin of repulsion of the origin.

1.4.4 Collinear set and singular dynamics

Consider the single–input dynamics

$$\frac{\mathrm{d}x}{\mathrm{d}t}(t) = X(x(t)) + u(t)Y(x(t)), \quad 0 \leq u \leq 1, \tag{1.13}$$

where Y is one of the vector field Y_1, Y_2 associated to a probiotic or an antibiotic agent.

Collinear set

It is defined by $C = \{x_e : \exists u_e \text{ constant such that } X(x_e) + u_e Y(x_e) = 0\}$ and x_e is a forced equilibrium. The control u_e is said feasible if $0 \leq u_e \leq 1$.

Singular dynamics

In the $3d$ case, the singular control can be computed as a feedback [3]. This is given by the following proposition.

Proposition 7. *Consider the single–input control system* (1.13) *in* $\mathbb{R}^3$*. Introduce the following determinants :*

- $D = \det(Y, [Y, X], [[Y, X], Y])$,
- $D' = \det(Y, [Y, X], [[Y, X], X])$,
- $D'' = \det(Y, [Y, X], X)$.

Then the singular control with minimal order is given by the feedback:

$$u_s(x) = -\frac{D'(x)}{D(x)},$$

so that the singular dynamics is defined by :

$$\frac{\mathrm{d}x}{\mathrm{d}t} = X_s(x) = X(x) - \frac{D'(x)}{D(x)}\, Y(x).$$

The sets $D'' = 0$, $DD'' > 0$ and $DD'' < 0$ are foliated respectively by exceptional, hyperbolic and elliptic arcs and are invariant for the integral curves of the vector field $X_s(x)$.

Computations

One has the following expressions of D, D', D'' in the original coordinates :

$$\begin{aligned}
D(x)/x_1x_2x_3 = \\
&\left(\varepsilon_1^2 x_1 a_{21} + \varepsilon_1\left(\varepsilon_2\left(x_2a_{22} - x_1a_{11}\right) + \varepsilon_3 x_3 a_{23}\right) - \varepsilon_2\left(\varepsilon_2 x_2 a_{12} + \varepsilon_3 x_3 a_{13}\right)\right) \\
&\left(\varepsilon_1^2 x_1 a_{31} + \varepsilon_2^2 x_2 a_{32} + \varepsilon_3^2 x_3 a_{33}\right) + \left(\varepsilon_1^2 x_1 a_{11} + \varepsilon_2^2 x_2 a_{12} + \varepsilon_3^2 x_3 a_{13}\right)\left(\varepsilon_2^2 x_2 a_{32}\right. \\
&\left. + \varepsilon_3\varepsilon_2\left(x_3a_{33} - x_2a_{22}\right) - \varepsilon_3^2 x_3 a_{23} + \varepsilon_1 x_1\left(\varepsilon_2 a_{31} - \varepsilon_3 a_{21}\right)\right) \\
-&\left(\varepsilon_1^2 x_1 a_{21} + \varepsilon_2^2 x_2 a_{22} + \varepsilon_3^2 x_3 a_{23}\right)\left(\varepsilon_1^2 x_1 a_{31} + \varepsilon_1\left(\varepsilon_2 x_2 a_{32} + \varepsilon_3\left(x_3a_{33} - x_1a_{11}\right)\right)\right. \\
&\left. - \varepsilon_3\left(\varepsilon_2 x_2 a_{12} + \varepsilon_3 x_3 a_{13}\right)\right),
\end{aligned}$$

$$
\begin{aligned}
&D'(x)/x_1x_2x_3 = \\
&\big(-\varepsilon_1^2x_1\ a_{21}+\varepsilon_1\left(\varepsilon_2\left(x_1a_{11}-x_2a_{22}\right)-\varepsilon_3x_3a_{23}\right)+\varepsilon_2\left(\varepsilon_2x_2a_{12}+\varepsilon_3x_3a_{13}\right)\big)\\
&\big(\varepsilon_2x_2\big(x_1a_{12}a_{31}-a_{32}\big(x_1a_{21}+x_3\big(a_{23}-a_{33}\big)+r_2\big)\big)-\varepsilon_1x_1\big(r_1a_{31}+x_3\left(a_{13}-a_{33}\right)a_{31}\\
&+x_2\big(a_{12}a_{31}-a_{21}a_{32}\big)\big)+\varepsilon_3x_3\left(-r_3a_{33}+x_1a_{31}\left(a_{13}-a_{33}\right)+x_2a_{32}\left(a_{23}-a_{33}\right)\right)\big)\\
&+\big(\varepsilon_2^2\left(-x_2\right)a_{32}+\varepsilon_3\varepsilon_2\left(x_2a_{22}-x_3a_{33}\right)+\varepsilon_3^2x_3a_{23}+\varepsilon_1x_1\left(\varepsilon_3a_{21}-\varepsilon_2a_{31}\right)\big)\\
&\big(-\varepsilon_1x_1\left(r_1a_{11}+x_2a_{12}\left(a_{11}-a_{21}\right)+x_3a_{13}\left(a_{11}-a_{31}\right)\right)+\varepsilon_2x_2\big(x_3a_{13}a_{32}\\
&-a_{12}\big(x_1\left(a_{21}-a_{11}\right)+x_3a_{23}+r_2\big)\big)-\varepsilon_3x_3(a_{13}\left(x_1\left(a_{31}-a_{11}\right)+x_2a_{32}+r_3\right)\\
&-x_2a_{12}a_{23})\big)-\big(-\varepsilon_1^2x_1a_{31}+\varepsilon_1\left(\varepsilon_3\left(x_1a_{11}-x_3a_{33}\right)-\varepsilon_2x_2a_{32}\right)+\varepsilon_3(\varepsilon_2x_2a_{12}\\
&+\varepsilon_3x_3a_{13})\big)\big(\varepsilon_1x_1\left(x_3a_{23}a_{31}-a_{21}\left(x_3a_{13}+x_2\left(a_{12}-a_{22}\right)+r_1\right)\right)+\varepsilon_2x_2\\
&\big(-r_2a_{22}+x_1a_{21}\left(a_{12}-a_{22}\right)+x_3a_{23}\left(a_{32}-a_{22}\right)\big)+\varepsilon_3x_3(x_1a_{13}a_{21}-a_{23}(x_1a_{31}\\
&+x_2\left(a_{32}-a_{22}\right)+r_3))\big),
\end{aligned}
$$

$$
\begin{aligned}
&D''(x)/x_1x_2x_3 = \\
&\big(-\varepsilon_1^2x_1a_{21}+\varepsilon_1\left(\varepsilon_2\left(x_1a_{11}-x_2a_{22}\right)-\varepsilon_3x_3a_{23}\right)+\varepsilon_2\left(\varepsilon_2x_2a_{12}+\varepsilon_3x_3a_{13}\right)\big)\\
&\left(x_1a_{31}+x_2a_{32}+x_3a_{33}+r_3\right)+\big(-\varepsilon_2^2x_2a_{32}+\varepsilon_3\varepsilon_2\left(x_2a_{22}-x_3a_{33}\right)+\varepsilon_3^2x_3a_{23}\\
&+\varepsilon_1x_1\big(\varepsilon_3a_{21}-\varepsilon_2a_{31}\big)\big)\left(x_1a_{11}+x_2a_{12}+x_3a_{13}+r_1\right)+\big(\varepsilon_1^2x_1a_{31}+\varepsilon_1\big(\varepsilon_2x_2a_{32}\\
&+\varepsilon_3\left(x_3a_{33}-x_1a_{11}\right)\big)-\varepsilon_3\left(\varepsilon_2x_2a_{12}+\varepsilon_3x_3a_{13}\right)\big)\left(x_1a_{21}+x_2a_{22}+x_3a_{23}+r_2\right).
\end{aligned}
$$

Remark 2. Similar computations hold in the bi-input case with $Y(x) = \mathrm{span}\{Y_2(x), Y_2(x)\}$. Note that $Y(x)$ is integrable since $[Y_1, Y_2] = 0$. Such computations are necessary to identify the singular dynamics, which have to be avoided because of strong accessibility problems, see [8].

1.4.5 Computational path as a medical protocol

- Classify the eight equilibria computing the spectrum of the Jacobian matrix evaluated at these points.
- The objective function to minimize is $x \to x_1(T)$, which can be reformulated as a problem of reaching the surface $x_1(t_f) \leq x_1^{\min}$ in minimum time where $x_1^{\min}$ is a given threshold, representing the level from which the detection of the infection is possible.

We shall take into account various constraints on the system in the framework of sampled-data control :

- *Infection constraints.* The infected population has to be lower than a given threshold $x_1^{\max}$, representing the maximum level of infection.
- *Logistic constraints.* The therapy consists of delivering treatment on specific times intervals $[t_i, t_{i+1}]$, where the duration $t_{i+1} - t_i$ is bigger than an interpulse $t_{i+1} - t_i \geq I_m$ e.g. $I_m = 1$ day. The controls $u_i, i = 1, 2$ are constant on each interpulse and are bounded by some constants m_i.

- At final time T of the caring therapy (e.g. $T = 40$ days) it is required that the final point $x(T)$ is in a stability domain of a forced equilibrium point denoted x_{ef} associated to an admissible control.
- Additional L^2–constraints can be added to take into account the cost or the total amount of available drug e.g. antibiotic.

1.4.6 Numerical simulations

The previous geometric analysis leads to design direct numerical schemes or semi-direct scheme based on NMPC method (Nonlinear Model Predictive Control) [18].

We present preliminary results on the $3d$ Lotka Volterra system (1.12) with $X(x) = \mathrm{diag}x(r - Ax)$, $r = (1,1,1)^\intercal$, $A = \begin{pmatrix} 1 & \alpha & \beta \\ \beta & 1 & \alpha \\ \alpha & \beta & 1 \end{pmatrix}$ and in the case $\alpha+\beta > 2$, $\alpha < 1$. This implies that the carrying simplex is the plane $x+y+z = 3/(1+\alpha+\beta)$ and the interior equilibrium exists and is an unstable focus (see Table 1.1).

Equilibria and stability

The spectrums of the Jacobians $\frac{\partial X}{\partial x}$ evaluated at the eight free equilbria are given in Table 1.1.

Free equilibria $X(x_e) = 0$	Spectrum spec $\left(\frac{\partial X}{\partial x}_{\mid x=x_e}\right)$
$(0,0,0)$	$\{1,1,1\}$
$(0,0,1)$, $(1,0,0)$, $(0,1,0)$	$\{-1, 1-\alpha, 1-\beta\}$
$(\frac{1}{\alpha+\beta+1}, \frac{1}{\alpha+\beta+1}, \frac{1}{\alpha+\beta+1})$	$\left\{-1, \frac{\alpha+\beta-2-i\sqrt{3}\lvert\alpha-\beta\rvert}{2(\alpha+\beta+1)}, \frac{\alpha+\beta-2+i\sqrt{3}\lvert\alpha-\beta\rvert}{2(\alpha+\beta+1)}\right\}$
$(0, \frac{\alpha-1}{\alpha\beta-1}, \frac{\beta-1}{\alpha\beta-1})$, $(\frac{\beta-1}{\alpha\beta-1}, 0, \frac{\alpha-1}{\alpha\beta-1})$ $(\frac{\alpha-1}{\alpha\beta-1}, \frac{\beta-1}{\alpha\beta-1}, 0)$	$\left\{\frac{(\alpha-1)(\beta-1)}{\alpha\beta-1}, -1, \frac{-\alpha^2+\alpha\beta+\alpha-\beta^2+\beta-1}{\alpha\beta-1}\right\}$

Table 1.1. Spectrum of the Jacobian matrix of X evaluated at the eight equilibria of the May and Leonard model.

Optimization problem

To reduce the x_1 population in the biological frame, where stability of the final point $x_1(T)$ is required we proceed as follows.

1. Prior to the infection, we assume that the patient is in a healthy stable state represented as a stable equilibrium point (x_{20}, x_{30}) of a two-dimensional Lotka–Volterra system.
2. Suppose the patient got infected by a pathogen agent at time $t = 0$. At time $t > 0$ its state is represented as a $3d$ vector $(x_1(t), x_2(t), x_2(t))$ with $x(0) = (x_{10}, x_{20}, x_{30})$, $x_{10} \gg x_1^{\min} > 0$. This vector is governed by a $3d$ Lotka-Volterra system.
3. From $x(0)$, we accelerate the evolution of the state to the variety Π. This is formulated as a minimum time control problem $3d$ Lotka–Volterra system using probiotics only.
4. Finally, we reach, in minimum time using antibiotics, an healthy region $N : x_1(T) \leq k\, x_1^{\min}$, where $k < 1$ is a scaling factor. To ensure that the final point is in a stable healthy region, the stability can be obtained by a pole placement method [11].

Direct method

We illustrate our previous four steps protocol by computing a trajectory $x_{ref}(.)$ using the Bocop software [2] with $\alpha = 0.2$, $\beta = 2$.

The point $(x_2(0), x_3(0)) = (0.1, 0.1)$ corresponds to a forced stable equilibrium of the $2d$ Lotka–Volterra system : it is a point on the collinearity set associated to the control $u_e = 0.75$ and for suitable values of $\varepsilon_1, \varepsilon_2$ and, where the eigenvalues of the Jacobian matrix

$$\frac{\partial}{\partial x}(X(x) + uY(x))_{|x=(x_2(0),x_3(0)),u=u_e}$$

have strictly negative real parts.

At time $t = 0$, a pathogen agent is measured with $x_1(0) = 0.1 =: x_1^{\min}$. Then in Phase 1 we accelerate the evolution of the state (x_1, x_2, x_3), governed by the $3d$ Lotka–Volterra system

$$\begin{pmatrix} \dot{x}_1(t) \\ \dot{x}_2(t) \\ \dot{x}_3(t) \end{pmatrix} = \mathrm{diag}x \left(\begin{pmatrix} 1 \\ 1 \\ 1 \end{pmatrix} - \begin{pmatrix} 1 & \alpha & \beta \\ \beta & 1 & \alpha \\ \alpha & \beta & 1 \end{pmatrix} x(t) + u(t) \begin{pmatrix} 1.5 \\ 0.4 \\ 1 \end{pmatrix} \right),$$

towards the flat carrying simplex $\Pi : x + y + z = 1/(1 + \alpha + \beta)$ by using probiotics only.

When we are close enough to Π, Phase 2 is initiated and we minimize the time to reach the healthy region $x_1(T) < x_1^{\min}/2$, using antibiotics only with $Y(x) = \mathrm{diag}x\,(-0.5, -1.4, -1)^\intercal$. The trajectory resulting from these two phases is displayed in Fig.1.6.

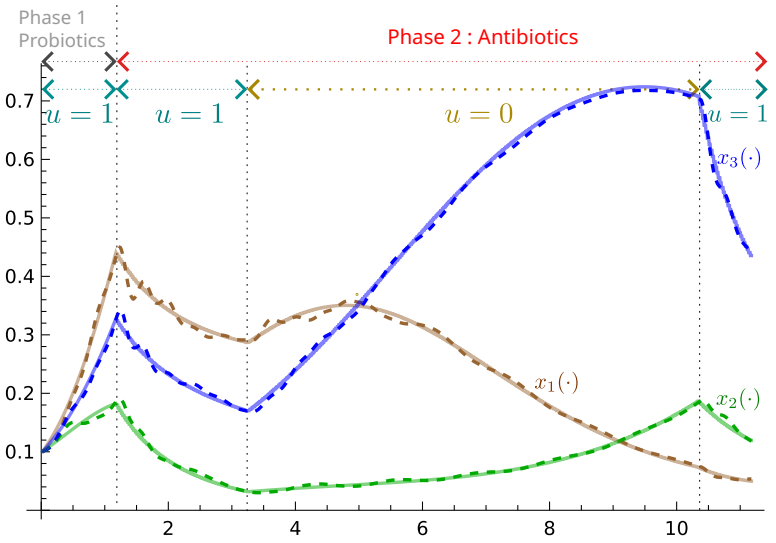

Fig. 1.6. *(Continuous curves)* Reference trajectory x_{ref} computed with a direct method on a $3d$ totally competitive Lotka–Volterra model following the four steps protocol given in section 1.4.5. *(Dashed curves)* Tracking trajectory obtained via a NMPC tracking method on the reference trajectory.

NMPC tracking

A predictive controller model is constructed through the minimization of a cost function involving the state and control inputs over a finite time horizon, with consideration for constraints on both inputs and states. The feedback control input has a piecewise affine structure of the form $u_f = -K\,x + \Lambda$, which can be easily deployed in microcontrollers for fast processes.

First, we start by constructing a discrete-time approximation of the bi-input system (1.12) using a Tustin bilinear transformation with sampling period $\tau > 0$. Let $x_{ref}(\cdot)$ be a reference trajectory. Define the cost

$$J(x, u_f) := \sum_{k=1}^{\eta} \|e(k)\|_2^2 + \|\Delta u_f(k)\|_2^2 + \kappa e(k)^\intercal \Delta u_f(k),$$

where η is the horizon, $e(k) = x_{ref}(k) - x(k)$ is the predicted error, $\Delta u_f(k) = u_f(k) - u_f(k-1)$ is the incremental feedback control input and $\kappa > 0$ is a parameter.
The feedback control is computed by minimizing the cost J subject to the discrete dynamic constraint obtained with the Tustin transformation and such that each control component is in $[0, 1]$.

Plugging the feedback control in the control dynamics (1.12) yields a closed loop system, robust with respect to perturbations and uncertainties on the state x.

Numerical results.

Take the trajectory $x_{ref}(\cdot)$, computed with the direct method, as a reference trajectory. The feedback control is computed with the following NMPC parameters : $\tau = 0.005$, $\eta = 5$, $\kappa = 0.002$ and the parameters of the dynamics (1.12) are $\epsilon_1 = (1.5, 0.4, 1.0)^\intercal$, $\epsilon_2 = (0.5, -1.4, -1.0)^\intercal$, $\alpha = 0.2$ and $\beta = 2$. Time evolution of the trajectory of the resulting closed loop system is displayed in Figure 1.6 as dashed curves showing the ability to track the reference signal.
Note that we can accelerate the recovery by computing the feedback control with a predicted error of the form $e(k) = x_{ref}(k+p) - x(k)$ for some integer $p > 1$.

1.5 Conclusion

This article presents briefly a combination of geometric and numerical methods to analyze the problem of reduction of a complex microbiote by a pathogenic agent. It leads to robust optimal control schemes to quantify the effect of different medical protocols. Computation are presented for the $2d$-system and for $3d$-totally competitive Lotka–Volterra models.

References

1. S. Baigent, Geometry of carrying simplices of 3-species competitive Lotka-Volterra systems, *Nonlinearity*, **26**, (2013) 1001–1029.
2. Team Commands, Inria Saclay, BOCOP: an open source toolbox for optimal control, http://bocop.org, 2017.
3. B. Bonnard, M. Chyba, The role of singular trajectories in control theory, Springer Verlag, New York, 2003, 357 pages.
4. B. Bonnard, G. Launay, M. Pelletier, Classification générique de synthèses temps minimales avec cible de codimension un et applications, *Annales de l'I.H.P. Analyse non linéaire*, **14** no.1 (1997), 55–102.
5. B. Bonnard, J. Rouot, Towards Geometric Time Minimal Control without Legendre Condition and with Multiple Singular Extremals for Chemical Networks, *Advances in Nonlinear Biological Systems, Modeling and Optimal Control, AIMS on applied Maths*, **11** (2021), 1–34.
6. B. Bonnard, J. Rouot, Optimal Control of the Controlled Lotka-Volterra Equations with Applications - The Permanent Case, *SIAM J. Appl. Dyn.*, **22** no. 4 (2023), 2761–2791.
7. B. Bonnard, J. Rouot, Feedback Classification and Optimal Control with Applications to the Controlled Lotka-Volterra Model, Preprint 2023: hal-03861565.

8. B. Bonnard, J. Rouot, C. Silva, Geometric Optimal Control of the Generalized Lotka-Volterra Model of the Intestinal Microbiome, Accepted for publication in OCAM (2024) : hal-03861565.
9. V.G. Boltyanskii, Sufficient conditions for optimality and the justification of the dynamic programming method, *SIAM J. Control*, **4** (1966), 326–361.
10. P. Brunovský, Existence of regular synthesis for general control problems, *J. Differential Equations*, **38** no. 3 (1980), 317–343.
11. H. Hermes, On the Synthesis of a Stabilizing Feedback Control via Lie Algebraic Methods, *SIAM J. Control Optim.*, **18**, no. 4, (1980) 352–361.
12. J. Hofbauer, J. W.-H. So, Multiple limit cycles for three dimensional Lotka-Volterra equations, *Applied Math. Lett.*, **7**, no. 6, (1994) 65–70.
13. E.W. Jones, P. S. Clarcke, J. M. Carslon, Navigation of outcome in a generalized Lotka–Volterra model of the microbiome, *Advances in Nonlinear Biological Systems, Modeling and Optimal Control, AIMS on applied Maths*, **11** (2021), 97–117.
14. I. Kupka, Geometric theory of extremals in optimal control problems. I. The fold and Maxwell case, *Trans. Amer. Math. Soc.*, **299** no.1 (1987), 225–243.
15. G. Launay, M. Pelletier, The generic local structure of time-optimal synthesis with a target of codimension one in dimension greater than two, *Journal of Dynamical and Control Systems*, **3**, no. 165 (1997).
16. S. Nikitin, Piecewise-Constant Stabilization, *SIAM J Control Optim.*, **37**, no. 3, (1999) 911–933.
17. L.S. Pontryagin, V.G. Boltyanskii, R.V. Gamkrelidze, E.F. Mishchenko, The mathematical theory of optimal processes, *Oxford, Pergamon Press*, 1964, 362 pages.
18. J. Rawlings, D. Mayne, M. Diehl, Model Predictive Control: Theory, Computation, and Design, Santa Barbara, CA: Nob Hill, 2017, 819 pages.
19. H. Schättler, U. Ledzewicz, Optimal control for mathematical models of cancer therapies. An application of geometric methods, *Interdisciplinary Applied Mathematics*, **42**. Springer, New York, 2015, 496 pages.
20. R.R. Stein, V. Bucci, N.C. Toussaint, C.G. Buffie, G. Rätsch, E.G. Pamer, et al., Ecological modelling from time-series inference: insight into dynamics and stability of intestinal microbiota, *PLos Comp. Biology*, **9** no. 12 (2013).
21. V. Volterra, Leçons sur la théorie mathématique de la lutte pour la vie, Les Grands Classiques Gauthier-Villars. Éditions Jacques Gabay, Sceaux, 1990, 215 pages.